33RD INTERNATIONAL COSMIC RAY CONFERENCE, RIO DE JANEIRO 2013
THE ASTROPARTICLE PHYSICS CONFERENCE

Precision measurement of the proton flux with AMS

S. HAINO[1] ON BEHALF OF THE AMS-02 COLLABORATION.

[1] *National Central University*

sadakazu.haino@cern.ch

Abstract: The proton flux in rigidities from 1 GV to 1.8 TV has been measured by AMS during the first two years of operation on the ISS. In the low rigidity region below 20 GV, the flux is determined every day with the statistical error less than 1 %. We have observed a gradual change of the flux due to the solar modulation as well as a drastic change after large solar flares. In the rigidity region from 20 GV to 100 GV our data are consistent with the previous measurements by magnetic spectrometers. In the high rigidity region above 100 GV the spectrum is consistent with a single power law spectrum and shows no fine structure nor break.

Keywords: AMS-02, Cosmic-ray proton, Magnetic spectrometer

1 Introduction

Protons are the most abundant particles in cosmic rays from space. Their absolute flux and spectral shape are fundamental data to discuss the origin and the propagation history of the cosmic rays in the Galaxy as well as to study the solar phenomena. Recently there has been a strong interest in the spectral shape above 100 GeV. In this paper we present the accurate determination of the proton flux.

2 AMS detector

AMS [1] is a magnetic spectrometer consisting of a permanent magnet which produces a field of 1.4 kG [2], nine layers of silicon Tracker which has a maximum track path length of 3 m [3], four planes of time of flight (TOF) counters which determines the particle direction and provides the velocity measurement and trigger [4], and several other particle detectors [1]. Particle rigidity, which is defined as the momentum divided by charge, is measured by fitting the three dimensional trajectory bent in the magnetic field and precisely measured by the tracker. The maximum detectable rigidity (MDR) is estimated as about 2 TV for protons [5, 6]. AMS was installed on the International Space Station (ISS) on 19 May 2011 to conduct a unique long duration mission ($\sim$20 years) of fundamental physics research in space.

3 Data sample and exposure time

We have analyzed data taken from 19 May 2011 to 19 May 2013 (two years). For each second out of 6.3×10^7, the global status of AMS is defined with several parameters. The exposure time period is selected with second-by-second basis as follows:

- AMS is in the nominal data taking status,
- AMS vertical axis is within 25° of the Earth zenith axis, and
- the measured rigidity is required to exceed by a factor 1.2 of the maximal Stoermer cutoff[7].

The total exposure time depends on the measured rigidity and it is 1.52×10^6 seconds for 1 GV and rapidly increases as a function of rigidity. For rigidities above 25 GV it is constant and 5.12×10^7 seconds, which corresponds to an overall average live time fraction of 81.6% for two years.

4 Event selection

In order to have the highest possible rigidity resolution, we selected events with at least one full span track in the tracker, where the full span track is defined to have hits in both outer most planes (layer 1 and 9) for the rigidity measurement.

Preselection

For the first step of this analysis, events are requested to have:

- the velocity measured by at least three TOF layers being consistent with down going particles, and
- the linearly extrapolated trajectory of the TOF hit positions passing both tracker layer 1 and 9,

Proton track selection

Proton candidates are selected among the preselected samples to have:

- at least one track reconstructed in the tracker with four planes inside the magnet bore, and
- the measured charge in the tracker consistent with $Z = 1$ particle,

Tracker charge is determined by multiple measurement of energy loss in up to nine layers of double sided silicon detectors [8]. As shown in Fig. 1, the $Z = 1$ charge selection efficiency is estimated with a pure proton sample selected by an independent charge measurement by TOF [9] and it is more than 99.9 % over the whole rigidity range.

Final sample selection

Proton events for the flux determination are selected to have:

- at least one track with measured hit positions in two coordinates both in layer 1 and 9, and

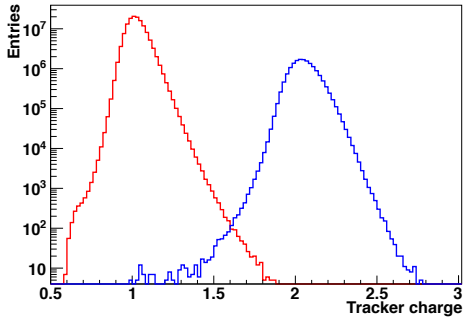

Fig. 1: Tracker charge distributions of proton and Helium pure sample selected an by independent charge measurement by TOF.

- Normalized χ^2 of the track fitting in the bending plane is less than 10,

and 3.03×10^8 events are selected.

4.1 Backgrounds

Protons are the most abundant particles in primary cosmic rays, but several possible backgrounds are studied:

4.1.1 Helium

As shown in Fig. 1, the probability that helium is misidentified as proton is estimated to be less than 0.1 % over the whole rigidity range with a pure helium sample selected by an independent charge measurement by TOF [9].

4.1.2 Pion

Pions produced in the atmosphere and in the material around AMS can contaminate proton sample. However we estimated that the pion contamination is less than 1 % in 1–2 GV after the measured rigidity is required to exceed by a factor 1.2 of the maximal Stoermer cutoff.

4.1.3 Electron and positron

Electrons are mostly rejected by requesting positive measured rigidity. The small migration of high energy electrons with misidentification of charge sign is negligible because the spectral index of electron is steeper than for protons [10]. In this analysis, we don't separate positrons from protons but the contribution is less than 1 %.

4.1.4 Deuteron

According to the previous measurement [11], the cosmic ray deuteron to proton ratio is 2∼3 % at 1 GV and decreases with increasing rigidity. In this analysis, we don't separate deuterons from protons. Therefore hydrogen nuclei have been selected in the proton sample.

5 Flux normalization

Assuming the flux over geomagnetic cutoff is isotropic, the differential proton flux, J is determined as a function of rigidity R as :

$$J(R) = \frac{N_{\rm obs}}{T_{\rm exp.} A_{\rm eff.} \varepsilon_{\rm trg.} \varepsilon_{\rm trk.} {\rm d}R} \qquad (1)$$

where:
– $N_{\rm obs}$ is the number of events obtained;
– $T_{\rm exp.}$ is the exposure time;
– $A_{\rm eff.}$ is the effective acceptance which includes both geometrical factor and the efficiency without large migration of energy due to hadronic interactions;
– $\varepsilon_{\rm trg.}$ is the trigger efficiency;
– $\varepsilon_{\rm trk.}$ is the selection efficiency of proton tracks ; and
– dR is the rigidity bin width.

5.1 Acceptance

The effective acceptance is estimated with a simulation technique [12]. Monte Carlo simulated events are produced by using a dedicated program developed based on the GEANT-4.9.4 package [13]. This program simulates electromagnetic and hadronic interactions of particles in the materials of AMS and generates detector responses. The digitized signals then undergo the same reconstruction as used for the data. The acceptance, $A_{\rm eff.}$ is obtained as :

$$A_{\rm eff.} = A_{\rm gen.} \times \frac{N_{\rm acc.}}{N_{\rm gen.}} \qquad (2)$$

where:
– $A_{\rm gen.}$ is a geometrical factor of the generation plane;
– $N_{\rm gen.}$ is the number of generated events, and
– $N_{\rm acc.}$ is the number of event which passed the preselection A.

We defined the generation plane with a 3.9×3.9 m^2 square surface on top of AMS, which corresponds $A_{\rm gen.} =$ 47.8 m^{2}sr. The obtained acceptance is constant above 10 GV and slightly (less than 5 %) depends on rigidity below 10 GV. The systematic error of 2.8 % is due to the uncertainty of energy dependence of the hadronic interaction probability.

5.2 Trigger efficiency

Different physics trigger conditions are implemented in the AMS-02 trigger logic to maximize the efficiency for different particle species while keeping a sustainable rate of the recorded events. In order to measure the trigger efficiency from data, 1/100 of the events with a coincidence of signals from at least 3 TOF planes are recorded as an unbiased sample. The trigger efficiency, $\varepsilon_{\rm trg.}$ is obtained as:

$$\varepsilon_{\rm trg.} = \frac{N_{\rm phys.}}{N_{\rm phys.} + 100 \times N_{\rm unb.}} \qquad (3)$$

where:
– $N_{\rm phys.}$ is the number of events that passed the proton selection and triggered with any of physics trigger conditions, and
– $N_{\rm unb.}$ is the number of events passed the proton selection and triggered as the unbiased sample. Fig. 2 shows the trigger efficiency as a function of measured rigidity. It is constant above 20 GV within 1 %. The systematic error of 1 % is due to the limited statistics of the unbiased trigger sample.

5.3 Track reconstruction efficiency

Track reconstruction efficiency is estimated as the ratio of number of events after the proton track selection over the number of events after the preselection and independent charge selection by TOF. The preselection sample includes the events passing out of the tracker sensitive area which

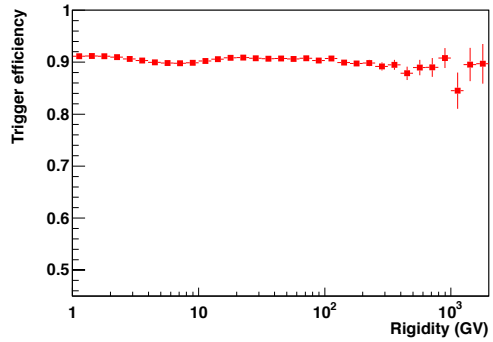

Fig. 2: Trigger efficiency as a function of measured rigidity.

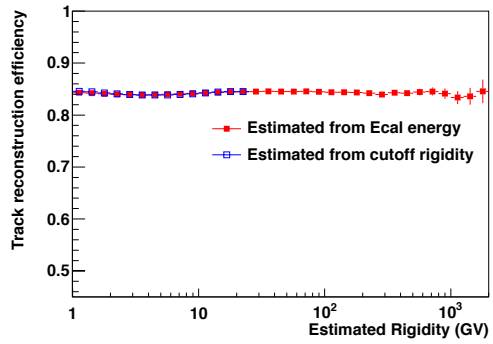

Fig. 3: Track reconstruction efficiency estimated among the preselection sample and TOF charge selection, which includes the events passing out of the tracker sensitive area (about 91 %). Red squares: The efficiency as a function of rigidity estimated by Ecal energy deposition. Blue open squares: The efficiency as a function of cutoff rigidity.

is about 91 %. Fig. 2 shows the track reconstruction efficiency as a function of rigidity estimated by the energy deposition in the Electro-magnetic calorimeter (Ecal). It is consistent with the rigidity estimated from the geomagnetic cutoff. The efficiency is constant within 1 % over the whole energy range. The systematic error of 1 % is due to the uncertainty of energy dependence.

5.4 Efficiency stability

As shown in Fig. 4, daily variations of the efficiencies, $\varepsilon_{\text{trg.}}$, and $\varepsilon_{\text{trk.}}$ for rigidities above 20 GV are estimated. $\varepsilon_{\text{trg.}}$ is constant within the statistical error of 0.7 %. For $\varepsilon_{\text{trk.}}$ the small increase on 24 July 2011 is because of the improvement of the tracker calibration and the small drop on 1 December 2011 is due to the loss of 3 % of tracker readout channels [14]. The lost channels are all for the non-bending coordinates so the impact on the rigidity measurement is negligibly small.

6 Binning and Unfolding

The rigidity binning is chosen according to the resolution estimated with the Monte Carlo simulation [5]. The normalized rigidity distribution of selected protons was corrected for the effects of bin-to-bin migration due to finite spectrometer resolution. The migration matrix is obtained with the Monte Carlo simulation and parametrized with t-

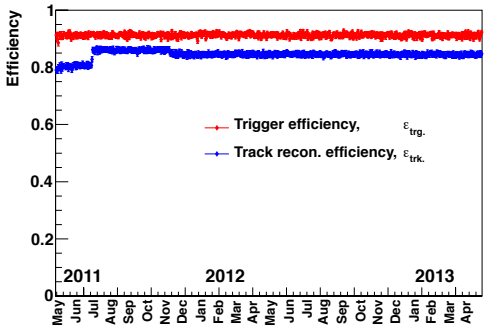

Fig. 4: Daily variation of the trigger efficiency ($\varepsilon_{\text{trg.}}$), and proton track efficiency ($\varepsilon_{\text{trk.}}$) for rigidities above 20 GV.

wo Gaussians. The incident differential proton flux was obtained by unfolding the measured flux based on Bayes' theorem [15]. The unfolding errors were estimated by changing the sigma of the resolution matrix by about 10 %, which corresponded to our test beam data extrapolation error to that energy, and allowing up to 1/20 TV^{-1} shift in the average inverse rigidity measurement, which corresponded to our current knowledge of tracker alignment using electron and positron samples [5, 6].

7 Error estimation

The statistical errors are always less than 1 % in the whole energy range.

The systematic errors on the flux normalization, $\sigma_{\text{norm.}}$ is estimated as $\sigma_{\text{norm.}} = 3.1$ % as :

$$\sigma_{\text{norm.}} = \sqrt{\sigma^2_{\text{acc.}} + \sigma^2_{\text{trg.}} + \sigma^2_{\text{trk.}}} \qquad (4)$$

where:
$\sigma_{\text{acc.}} = 2.8$ % is the error on the acceptance estimation;
$\sigma_{\text{trg.}} = 1.0$ % is the error on the trigger efficiency and;
$\sigma_{\text{trk.}} = 1.0$ % is the error on the proton track efficiency;
as discussed in previous sections.

As discussed in Section 6, the systematic error due to the unfolding, $\sigma_{\text{unfold.}}$ is estimated by changing the parametrization of migration matrix. It is less than 1 % below 100 GV and 5.4 % at 1 TV.

The total systematic errors are obtained as the quadratic sum of $\sigma_{\text{norm.}}$ and $\sigma_{\text{unfold.}}$ and it is 3.2 % below 100 GV and 6.3 % at 1 TV.

8 Daily flux variation

The flux below 30 GV is affected by solar activity. AMS can determine the proton flux every day with $\sim$1 % statistical error up to $\sim$20 GV. Fig. 5 shows the time variation of the flux with increasing rigidity bins between 1 and 100 GV, from blue to red. The fluxes at the beginning of observation are normalized to 1. We have observed the gradual decrease of flux in the low rigidity region ($R <\sim$10 GV) due to the solar modulation. The large spike on 7 March 2013 corresponds to the X5.4–class solar flare, which was the strongest solar eruption of the year 2012. We also observed the large Forbush decrease up to 30 GV, which lasted for about three weeks. Another spike on 17 May 2012 corresponds to the M5.1 solar flare and the first Ground

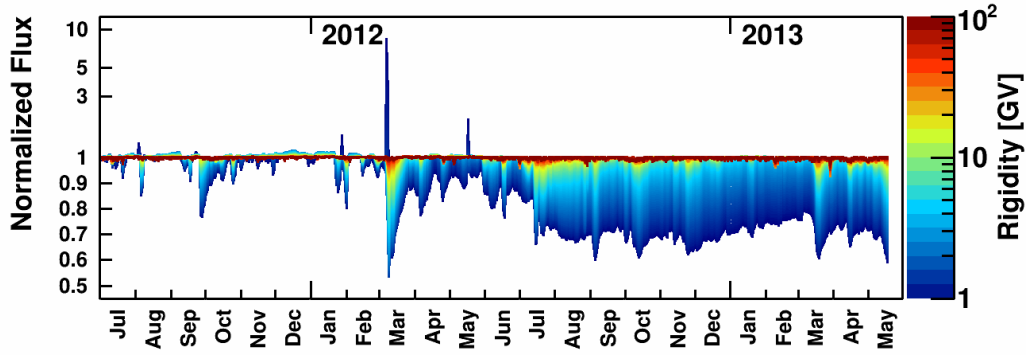

Fig. 5: Daily variation of normalized flux. We have observed the gradual decrease of flux in the low rigidity region ($R <\sim 10$ GV) as well as some spikes in $\sim$1 GV which correspond with solar events on 9 August 2011 (X6.9), 27 January 2012 (X1.7), 7 March 2013 (X5.4), and 17 May 2012 (M5.1).

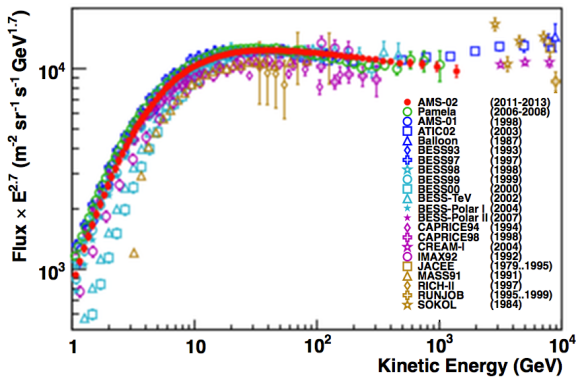

Fig. 6: The average proton flux over the two years of AMS-02 observation as a function of kinetic energy (E) multiplied by $E^{2.7}$ together with the previous experimental data [17]–[34].

Level Enhancement (GLE) event in Solar Cycle 24. We observed a few other small spikes which correspond to solar events on 9 August 2011 (X6.9) and 27 January 2012 (X1.7) and several Forbush decreases including the large one from 27 September 2011.

9 Result and conclusion

Fig. 6 shows the average proton flux over the two years of AMS-02 observation as a function of kinetic energy multiplied by corresponding bin central value [16] in the 2.7 power and compared with previous experimental data [17]–[34]. In the high energy region above 100 GeV the spectrum is consistent with a single power law spectra and shows no fine structure nor break.

Acknowledgements

This work has been supported by acknowledged person and institutions in [1].

References

[1] M. Aguilar et al., Phys. Rev. Lett 110 (2013) 141102.
[2] K. Luebelsmeyer et al., Nucl. Instrum. Methods A 654 (2011) 639.
[3] B. Alpat et al., Nucl. Instrum. Methods A 613 (2010) 207;
[4] A. Basili et al., Nucl. Instrum. Methods A 707 (2013) 99; V. Bindi et al., Nucl. Instrum. Methods A 623 (2010) 968.
[5] P. Zuccon et al., ICRC (2013) 1064.
[6] C. Delgado et al., ICRC (2013) 1260.
[7] C. Stoermer, The Polar Aurora (Oxford University, London, 1950).
[8] P. Saouter et al., ICRC (2013) 789.
[9] Q. Yan et al., ICRC (2013) 1097.
[10] S. Schael et al., ICRC (2013) 1257; B. Bertucci et al., ICRC (2013) 1267.
[11] J.Z. Wang et al., Astrophs. J. 564 (2002) 244.
[12] J.D. Sullivian et al., Nucl. Instrum. Methods 95 (1971) 5.
[13] S. Agostinelli et al., Nucl. Instrum. Methods A 506 (2003) 250.
[14] J. Bazo et al., ICRC (2013) 849.
[15] A. Kondor, Nucl. Instr. Meth. 216 (1983) 177; G. Agostini, Nucl. Instr. Meth. A 362 (1995) 487.
[16] G.D. Lafferty, T.R. Wyatt, Nucl. Instr. Meth. A 355 (1995) 541.
[17] O. Adriani, et al., Science, 332 (2011) 69; O. Adriani, et al., Astrophys. J. 765 (2013) 91.
[18] J. Alcaraz et al., Phys. Lett. B 490 (2000) 27.
[19] A.D. Panov et al., Bull. Russian Acad. Sci. 73 (2009) 564.
[20] M. Ichimura et al., Phys. Rev. D 48 (1993) 1949.
[21] Y. Shikaze et al., Astropart. Phys. 28 (2007) 154.
[22] T. Sanuki et al., Astrophys. J. 545 (2000) 1135.
[23] S. Haino et al., Phys. Lett. B 594 (2004) 35.
[24] K. Sakai et al., ICRC (2013) 974.
[25] M. Boezio et al., Astrophys. J. 518 (1999) 457.
[26] M. Boezio et al., Astropart. Phys. 19 (2003) 583.
[27] Y.S. Yoon et al., Astrophys. J. 728 (2011) 122.
[28] W. Menn et al., Astrophys. J. Lett. 533 (2000) 281.
[29] K. Asakimori et al., Astrophys. J. 502 (1998) 278.
[30] R. Bellotti et al., Phys. Rev. D 60 (1999) 052002.
[31] E. Diehl et al., APh 18, 487 (2003)
[32] M. Hareyama et al., J. Phys. Conf. 31 (2006) 159.
[33] I.P. Ivanenko et al., Proc. ICRC 2 (1993) 17
[34] D. Maurin et al., arxiv:1302.5525 (2013).